Eurasian Journal of Physics and Functional Materials

Volume 4 | Number 1

Article 6

Pages: 50 - 60

3-22-2020

Optimal technological modes of ion implantation and following annealing for forming thin nanosized films of silicides

A. S. Rysbaev
Tashkent State Technical University ,Uzbekistan

S. U. Irgashev
Termez State University ,Uzbekistan

A. S. Kasimov
Termez State University ,Uzbekistan

D. Sh. Juraeva
Termez State University ,Uzbekistan

J. B. Khujaniyazov
Tashkent State Technical University ,Uzbekistan

See next page for additional authors

Recommended Citation

Rysbaev, A. S.; Irgashev, S. U.; Kasimov, A. S.; Juraeva, D. Sh.; Khujaniyazov, J. B.; and Khudoyberdieva, M. I. (2020) "Optimal technological modes of ion implantation and following annealing for forming thin nanosized films of silicides," *Eurasian Journal of Physics and Functional Materials*: Vol. 4: No. 1, Article 6. DOI: https://doi.org/10.29317/ejpfm.2020040106

Optimal technological modes of ion implantation and following annealing for forming thin nanosized films of silicides

Authors

A. S. Rysbaev, S. U. Irgashev, A. S. Kasimov, D. Sh. Juraeva, J. B. Khujaniyazov, and M. I. Khudoyberdieva

Eurasian Journal of Physics and Functional Materials

2020, 4(1), 50-60

Optimal technological modes of ion implantation and following annealing for forming thin nanosized films of silicides

A.S. Rysbaev*[,1], S.U. Irgashev[2], A.S. Kasimov[2], D.Sh. Juraeva[2], J.B. Khujaniyazov[1], M.I. Khudoyberdieva[2]

[1]Tashkent State Technical University, Uzbekistan

[2]Termez State University, Uzbekistan

E-mail: rysbaev@mail.ru

DOI: **10.29317/ejpfm.2020040106**
Received: 05.02.2020 - after revision

The formation of nanosized films of silicides on the surface of Si (111) and Si (100) was studied by the method of low-energy ion implantation. The optimal technological modes of ion implantation and subsequent annealing for the formation of thin nanoscale films of silicides were determined. It is shown that the appearance of new surface superstructures is additional confirmation of the formation of thin silicide films with a single crystal structure.

Keywords: silicon, implantation, optimal structure, surface structure, films, spectrum of photoelectrons, zone energy diagram, nanoscale films, surface, silicide, single crystal, ion, dose.

Introduction

In recent years, considerable attention has been paid to the formation of thin single-crystal silicide films in silicon in connection with the prospect of their use in thermogenerators, thermoelectric batteries, heat radiation detectors, various sensors, as elements of functional integrated circuits for high-speed micro and nanoelectronic devices, and also as plasmonic waveguides for optoelectronic devices [1-5].

To form silicide films, we used the method of low-energy implantation of Ba^+ ions and alkali elements into a silicon single-crystal substrate that we developed and subsequent thermal annealing [6].

In [7, 8], the formation of β-$FeSi_2$/Si heterostructures by implanting Si (100) single crystals with low-energy Fe^+ ions with doses in the range of 10^{16} - 10^{17} cm^{-2} with subsequent processing of the implanted layers by pulsed laser or ion beams was demonstrated. Due to the small penetration depth of Fe^+ ions in Si during ion implantation and pulsed exposure (less than 0.2 pm), β-$FeSi_2$ layers were formed near the Si surface, which posed certain difficulties for the subsequent fabrication of LED structures [9].

Based on the analysis of existing publications on the formation of Si-β-$FeSi_2$-Si heterostructures, it can be argued that there is currently no work on the epitaxial growth of Si layers on β-$FeSi_2$ layers obtained by ion implantation. Si-$FeSi_2$-Si LED heterostructures were previously formed either by high-energy ion implantation (E > 200 keV) [1, 4] or by epitaxial growth of Si on a β-$FeSi_2$ layer obtained by reactive deposition of an Fe film on a Si substrate [9, 10].

Existing technologies of molecular beam epitaxy (MBE) and solid phase epitaxy (SFE) are aimed at the formation of sufficiently thick films in equilibrium in the form of bulk phases. This implies, with sufficient bulk of the films, a relatively high process temperature. At the same time, two factors are mainly used as growth regulators: sufficiently high deposition rate and substrate temperature during deposition or annealing. MBE and SFE technologies are well suited for homo- and heteroepitaxy of massive and thin-film isostructural materials.

In [11], the problem of controlling the growth of the first atomic layers of metal-semiconductor nanoheterostructures during physical deposition on a substrate in vacuum was considered. A low-temperature film growth process is proposed, based on the freezing of growing layers during the deposition process by maintaining a lower substrate temperature and using an atomic beam with a reduced thermal power. In this process, the special geometry of the deposition system is used, in which the distance between the source and the substrate is comparable or less than their size.

In [12, 13], a method was developed for the epitaxial growth in the solid phase of $CoSi_2$ films 5-10 nm thick on Si (111) substrates, including the 10^{-9} Pa formation of Co and Si atoms in vacuum from two sources, followed by coating the structure with an α-Si layer 1-2 nm thick and final annealing at 850-900 K for 10 min. Co and Si flows were selected in a ratio of 1:2.

In a recent work [14], to ensure such a growth process, the author proposed a new technology using low temperatures not only of the substrate, but also of the atomic beam, as well as other growth regulators, which allow one to create a given nonequilibrium state of ultrathin films.

Ion implantation allows the formation of both $CoSi_2$/Si structures and ternary structures of the Si/$CoSi_2$/Si type with the (100) and (111) orientations [15-18]. The applied energy of implanted Co^+ 200 keV ions, the optimal dose is $3.8 \cdot 10^{17}$ cm^{-2}. The obtained implanted $CoSi_2$ layers have excellent electrical properties: $\rho = 13$ $\mu Om \cdot cm$. However, this method has not yet found wide application. Nevertheless, to obtain ultrathin films and nanocrystals, it may be promising

to use the low-energy ion implantation method. This method has so far been used to modify the surface properties of materials of various nature, to obtain protective layers, ohmic contacts and for doping semiconductors. Along with this, the possibility of obtaining nanostructures of individual components during ion bombardment of inert gases, accelerated electrons and protons has been shown. In particular, Si nanostructures were created on the surface of SiO_2, and Ga nanostructures were created on the surface of GaAs. It should be noted that the electrophysical properties of the semiconductor can be significantly affected by other elements included in the solid solution formed on the basis of silicon. Outside solubility, this effect is much less noticeable [19]. Therefore, doping of silicon is carried out in amounts not exceeding the solubility limits of impurity elements in it. Thus, Si-based alloys are homogeneous solid solutions, most often they are substitution solutions, and less often, introductions and subtractions. Note that knowledge of the solubility of a substance and the nature of its change with temperature is necessary when creating silicon-based alloys and for a correct understanding of those changes in the properties of a semiconductor that occur during their heat treatment. When studying the annealing of the silicon – metal film system Ni, Pd, Cr, Au, Ag [20, 21], the formation of a disordered layer at the phase boundary was found: amorphous and elastically deformed regions are formed. The composition and depth of the disordered layers turned out to be different for the Pd-Si and Ni-Si systems. Similar phenomena were observed for samples of Cr-Si, Au-Si, however, for the case of Ag-Si, the disordered layer does not contain an amorphous region. An important conclusion was made that the presence of a disordered layer should lead to weakening of covalent bonds and stimulate diffusion and mutual diffusion processes [19]. Therefore, the formation of various phases and the properties of the heterogeneous Me-Si system depend on the formation conditions, i.e. from phase equilibrium of a given system. A detailed analysis [22] showed that the growth rates of all phases are interconnected and depend, in addition, on the diffusion characteristics of the substance inside these phases. In some cases, during the growth of solid phases, anomalous phenomena are observed on the surface (deviations from the parabolic law of phase growth, the absence of any of the phases in the diffusion zone, or its appearance only during very long diffusion anneals). Possible causes of such anomalies are discussed in the works [23, 24].

In this work, to form thin nanoscale silicide films, we propose a method of low-energy (E_0 =1 keV) high-dose ($\approx 10^{17}$ cm $^{-2}$) implantation of Li, K, Na, Rb, Cs, Ba ions in Si under ultrahigh vacuum ($\approx 10^{-8}$ Pa).

Experiment methodic

The experimental measurements were carried out in a device with a spherical mirror type analyzer with a decelerating field, which makes it possible to study the surface using Auger electron spectroscopy (AES), elastically scattered electron spectroscopy (ESES), photoelectron spectroscopy (PES) and slow electron diffraction (SED) at a pressure of residual gases of not more than 10^{-7} Pa [6]. Single

crystals of Si (111) and Si (100) n and p-type with a specific resistance of 6000 Ohm · cm were chosen as objects of study. In the technological chamber, the surface of the studied materials was cleaned by thermal heating, electron bombardment, and ion etching, as well as implantation of Ba ions and alkaline elements with energies of 0.5-5 keV, with different doses: from 10^{13} to $2 \cdot 10^{17}$ cm^{-2}. In addition, it was possible to obtain a clean surface with a chip in ultrahigh vacuum. The Si samples were purified by thermal heating in two stages: for a long time at a temperature of 1200 K for 60 min and for a short time at 1500 K for 1 min.

Results and Discussion

Based on the high-resolution systematic studies of SED, Auger electron spectroscopy (AES) and scanning electron microscopy (SEM) of studies of the surface region of Si during implantation of Li, K, Na, Rb, Cs and Ba ions with different energies and radiation doses, we The optimal modes of ion implantation (type, energy, dose) and subsequent thermal annealing (temperature, time) were determined for the formation of thin nanoscale metal films.

Table 1.
Optimal conditions for the formation of thin nanoscale films of barium silicides and alkaline elements.

Type of silicide / Parameters	LiSi	NaSi	KSi	RbSi	CsSi	BaSi
Source structure Si	111	100; 111	100	100; 111	100; 111	100; 111
Ion energy, keV	0.5-5	0.5-5	0.5-5	0.5-5	0.5-5	0.5-5
T annealing, K	900-1000	600-700	800-850	800-850	500-600	800-900
Thickness silicide, Å	50-110	45-100	35-95	30-90	40-90	35-85
Type of superstructure	4×4	4×4 1×1	2×1	2×4 2×2	2×8 2×2	2×2 1×1
The electrons energy E_P, eV	42	35; 43	49	35; 42	39; 30	38; 43
T restore the original structure, K	1400	1100	1200	1200	1000	1300

In the Table 1 shows the regimes of formation and types of surface superstructures of Ba silicides and alkaline elements formed upon heating of silicon samples implanted with 1 keV ions [25-28].

We note that we also observed surface superstructures during heating of samples implanted with high-energy ions (E_0 = 2 - 5 keV). The only difference was that the formation of surface structures required a longer (the greater, the greater the ion energy) annealing at the corresponding temperatures.

Depending on the type of the initial face of the silicon surface and the type of implantable ions of alkaline and alkaline-earth elements, the formation of various types of surface superstructures is observed. Earlier [25-28], we found that implantation of low-energy ions leads to disordering of the crystal structure up to complete amorphization of the surface region of Si (111) and Si (100). Critical doses of Si amorphization were determined. Starting with doses exceeding the amorphization dose, partial formation of new chemical compounds is observed. Short-term thermal annealing of ion-implanted Si samples leads to the formation of thin nanosized silicide films with new surface structures.

As a result of ion implantation and subsequent annealing, films of the following silicides are formed in the surface region of Si: LiSi, KSi, RbSi, CsSi, NaSi, and BaSi [29, 30].

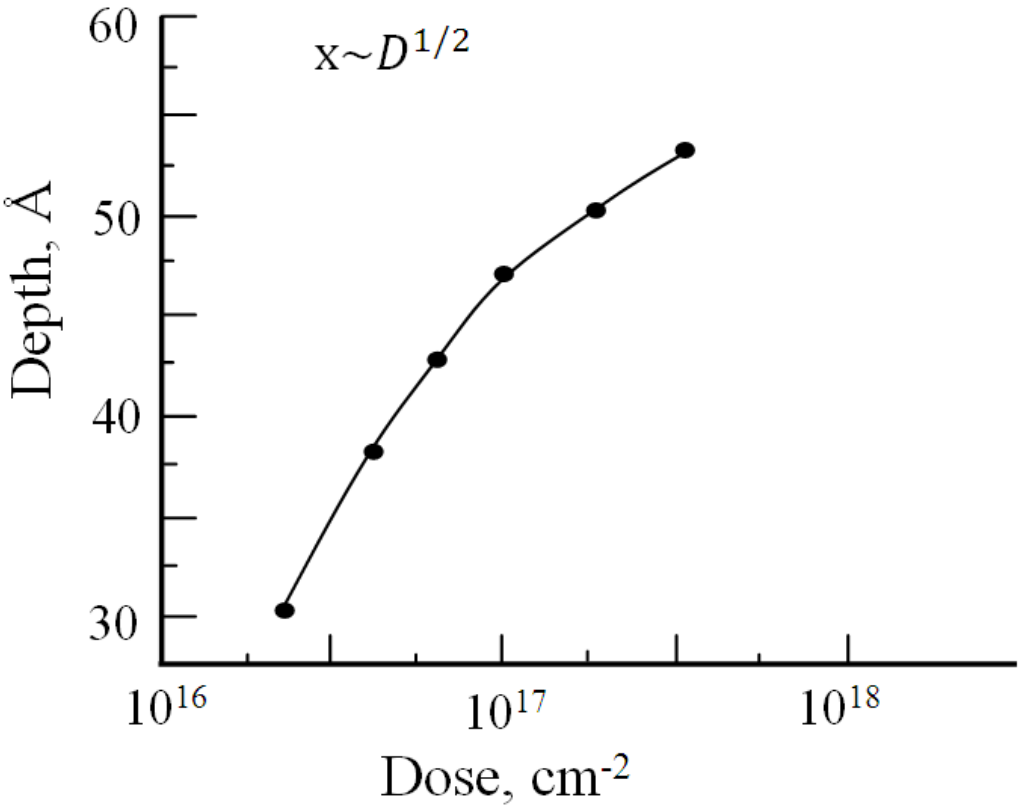

Figure 1. Dependence of the thickness of the RbSi x silicide film on the dose of D.

Experimental measurements of the thickness of silicide films showed that it grows with an increase in the energy of implanted ions; at a fixed ion energy, it also grows with an increase in dose of approximately $D^{1/2}$ (Figure 1). In Figure 1 shows the dependences of the thickness of the RbSi silicide film on the dose of D.

Measurement of the maximum range of Ba^+ ions and alkaline elements in Si(111) versus the energy of implanted ions showed that the range of ions increases almost linearly with increasing E_0 (Figure 2).

It was shown that implantation of Li^+, Rb^+, Cs^+, Na^+ ions with $E_0 = 1$ keV, a large dose in Si (111) and subsequent short-term heating at 600, 800, 500, 900 K, respectively, leads to the formation of silicides in the surface layer with the following structures: Si(111) - 4×4 Li (a); Si(111) - 2×2 Rb (b); Si(111) - 4×4 Cs (c),

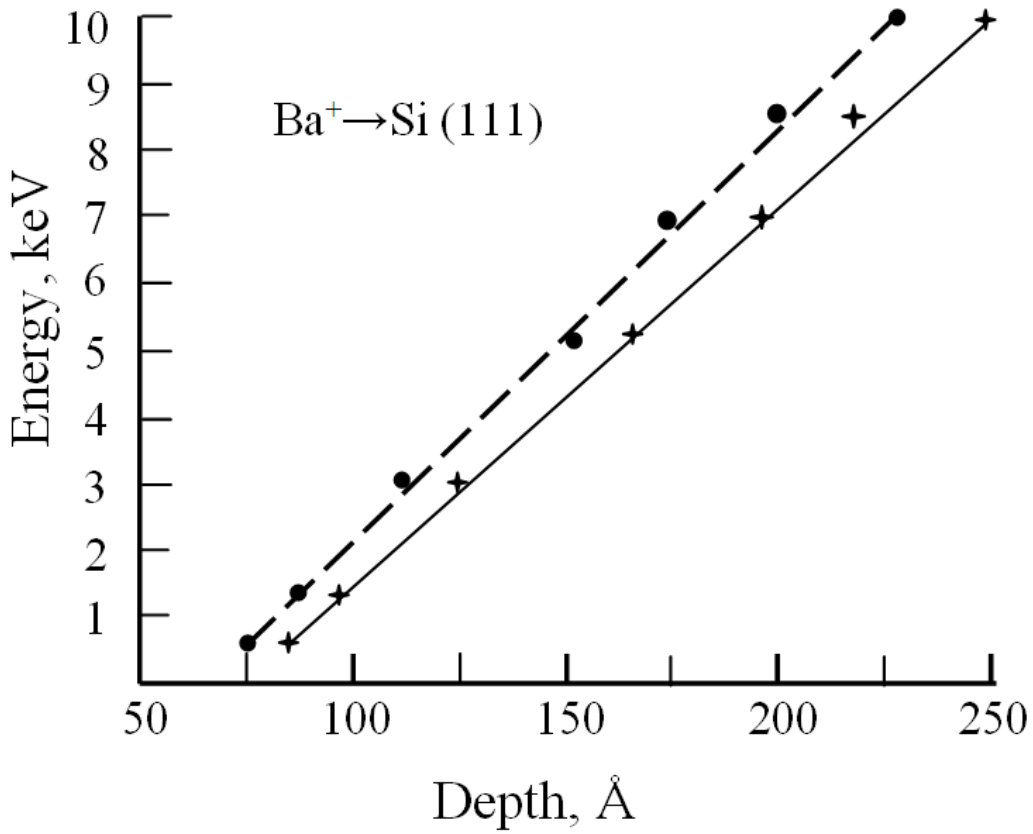

Figure 2. Dependences of the maximum range on the energy of implanted barium ions E_0 (solid curve - experiment, dashed curve - calculation).

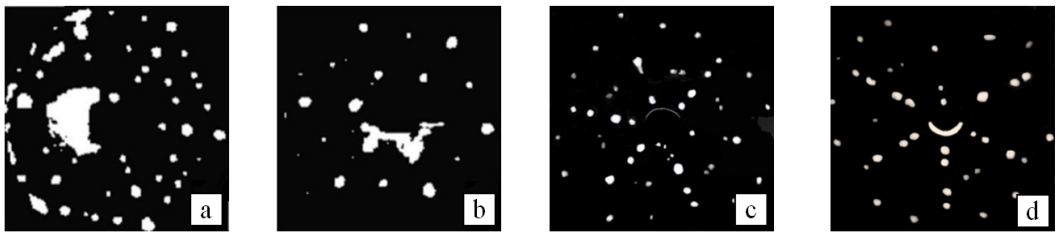

Figure 3. SED pictures obtained from a Si (111) surface implanted with Li, Rb, Cs, Na ions and subjected to short-term heating: Si(111)-4 × 4 Li (a); Si(111)-2 × 2 Rb (b); Si(111)-4 × 4 Cs (c), Si(111)-4 × 4 Na (d).

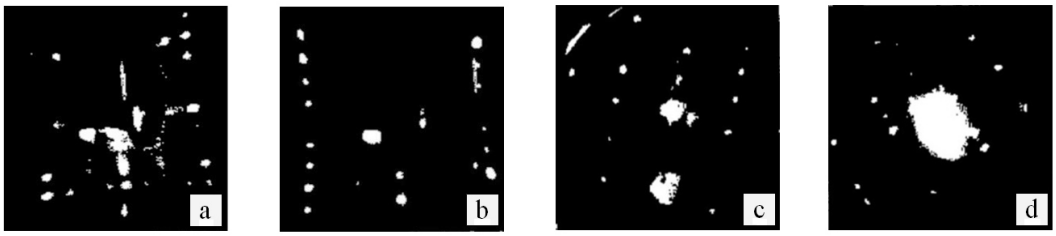

Figure 4. SED patterns obtained from a Si (100) surface implanted with Na, Rb, K, Cs ions and subjected to short-term heating: Si(100)-4 × 4 Na (a); Si(100)-2 × 4 Rb (b); Si(100)-2 × 1 K (c); Si(100)-2 × 8 Cs (d).

Si(111) - 4×4 Na (d) (Figure 3), and heating of Si(100) samples implanted with Na^+, Rb^+, K^+ and Cs^+ ions with $E_0 = 1$ keV leads to the formation of silicides with surface superstructures: Si(100) - 4×4 Na – (a); Si(100) - 2×4 Rb – (b); Si(100) - 2×1 K – (c); Si(100) - 2×8 Cs – (d) (Figure 4).

To study the changes in the electronic structure of the near-surface region of silicon as a result of ion implantation and subsequent annealing, we used the ESES

and PES methods. It is known [31] that the energy spectrum of photoelectrons taken at an incident photon energy of 10.8 eV reflects quite well the energy distribution of valence electrons of the sample under study.

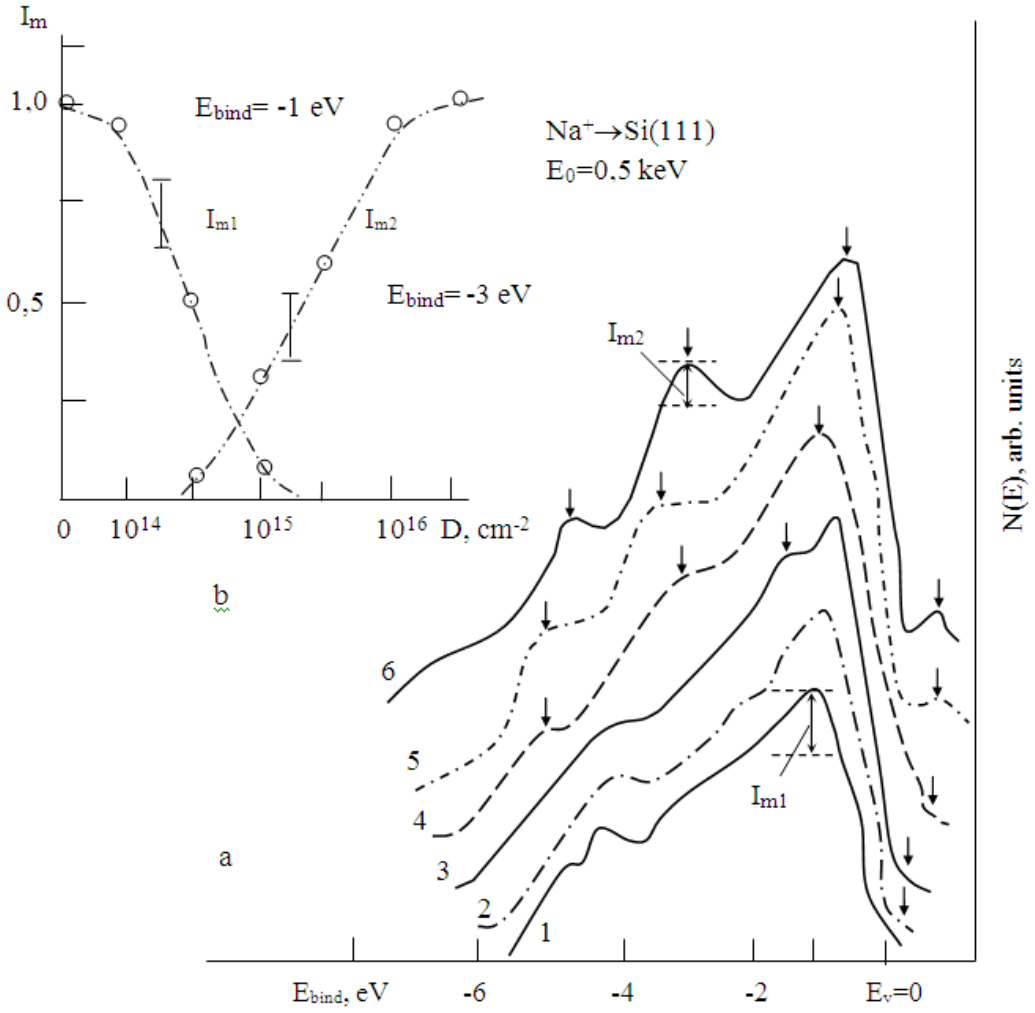

Figure 5. a – PES spectra for pure Si (curve 1) and Si implanted with Na ions with different doses of D, cm $^{-2}$: $1 \cdot 10^{14}$ (2), $5 \cdot 10^{14}$ (3), $5 \cdot 10^{15}$ (4), $1 \cdot 10^{16}$ (5), $6 \cdot 10^{16}$ (6). b – Is the change in the intensity of the peaks I_{m1} at E_{bind} = -1.0 eV and I_{m2} at E_{bind} = -3.0 eV from the radiation dose D.

In Figure 5a, the PES spectra are shown for pure silicon (curve 1) and Si implanted with Na^+ ions $E_0 = 0.5$ keV with different radiation doses D, cm $^{-2}$:10^{14} (curve 2); $5 \cdot 10^{14}$ (3); $5 \cdot 10^{15}$ (4); $1 \cdot 10^{16}$ (5) and $6 \cdot 10^{16}$ (6), taken at the incident photon energy of 10.8 eV.

It can be seen that in the photoelectron spectrum for a clean Si (111) surface there are maxima at E_{bind} ; -1.0; -2.7; -4.25; -4.8 eV, the position and shape of which satisfactorily coincides with the shape and position of the maxima of the density of states of valence electrons of silicon. With an increase in the dose of implantable Na^+ ions, the beginning of the PES spectrum shifts to the region of high energies, and the low-energy edge of the spectrum shifts to the region of lower energies, i.e. there is an expansion of the spectrum. Up to a dose of $D = 10^{15}$ cm $^{-2}$, the features characteristic of pure Si (111) are preserved in the PES spectrum.

With a further increase in D, the intensity of the peaks characteristic of pure Si decreases, the peaks associated with surface states disappear and new peaks

characteristic of the implanted impurity appear. In Figure 5b shows how the intensity I_{m1} of the Si (111) peak changes with E_{bind} = - 1.0 eV and the intensity I_2 of the new peak at E_{bind} = -3.0 eV characteristic of Si atoms chemically bonded to sodium atoms. It can be seen that the intensity of the silicon peak I_{m1} sharply decreases starting from $D = 1 \cdot 10^{14}$ cm^{-2} and completely disappears at $D = 2 \cdot 10^{15}$ cm^{-2}, and the peak I_{m2} appears at $D = 1 \cdot 10^{14}$ cm^{-2} and with a further increase in the ion dose Na increases, reaching saturation at $D = (6 - 8) \cdot 10^{16}$ cm^{-2}. As a result of implantation of Na^+ ions with E_0 = 0.5 keV and $D = 8 \cdot 10^{16}$ cm^{-2}, the quantum yield of photoelectrons increases by about 2 times, which is easy to see by comparing the areas under the curve of the energy distribution of photoelectrons for ion implanted (curve 6) and pure Si (curve 1). Our comparative analysis of the PES and ESES spectra of pure Si, silicon implanted with Na ions and a sodium film allowed us to peaks in curve 6 at E_{bind} = -0.6; -3.0; -4.9 and -7.0 eV consider to be characteristic of sodium silicide, and the peak at E_{bind} = -4.7 eV to be characteristic of silicon. The peak formation at E_{bind} = 0.9 eV is explained by the appearance at high doses of a new narrow subband of filled states near the bottom of the conduction band, which, as will be shown below, at $D \geq 6 \cdot 10^{16}$ cm^{-2} overlaps with the conduction band and leads to a narrowing of the Si forbidden band. The narrowing of the band gap can also be contributed by the so-called "gaffiry" of the bands, associated with strong disordering of the crystal lattice.

Based on the experimental data of PES and ESES, we have constructed approximate band energy diagrams for pure Si (Figure 6a), silicon implanted with Na^+ ions with E_0 = 0.5 keV (Figure 6b) and a NaSi film obtained after thermal annealing ion-implanted Si (Figure 6c).

The energy diagram for a clean single crystal surface of Si (111) is in good agreement with the data from the literature. The diagram shown in Figure 6b is characteristic of the amorphous phase of sodium silicide with an excess of sodium. As follows from the above diagram, implantation of Na ions in Si (111) with a high dose leads to a decrease in the work function due to both a decrease in the surface potential barrier (due to the adsorption of electropositive Na atoms on the Si surface and due to a shift in the level of E_f from the bottom band gap into the conduction band, that is, due to the formation of a sufficiently wide donor subband, Si implanted with Na ions exhibits a metallic character of conductivity. In addition, the distribution of valence electrons also changes - the maxima of the density of states to the upper edge of the valence band, while, as already noted, 70 - 80% of interstitial Na atoms form chemical compounds with silicon atoms. Annealing of ion-imilanthione Si at 900 K leads to the desorption of unbound Na atoms and to the formation of sodium silicide. There is no impurity subband in the diagram for NaSi, the band gap increases by 0.1 eV, and the E_f level is located near the bottom of the conduction band, i.e., sodium silicide is a semiconductor with an electronic type of conduction.

We constructed similar band energy diagrams for Si samples implanted with Li^+, K^+, Rb^+, Cs^+ ions and their silicides. Based on the constructed diagrams, we determined the parameters of the electronic structure of silicide films formed in the surface layer of Si by ion implantation (Table 2).

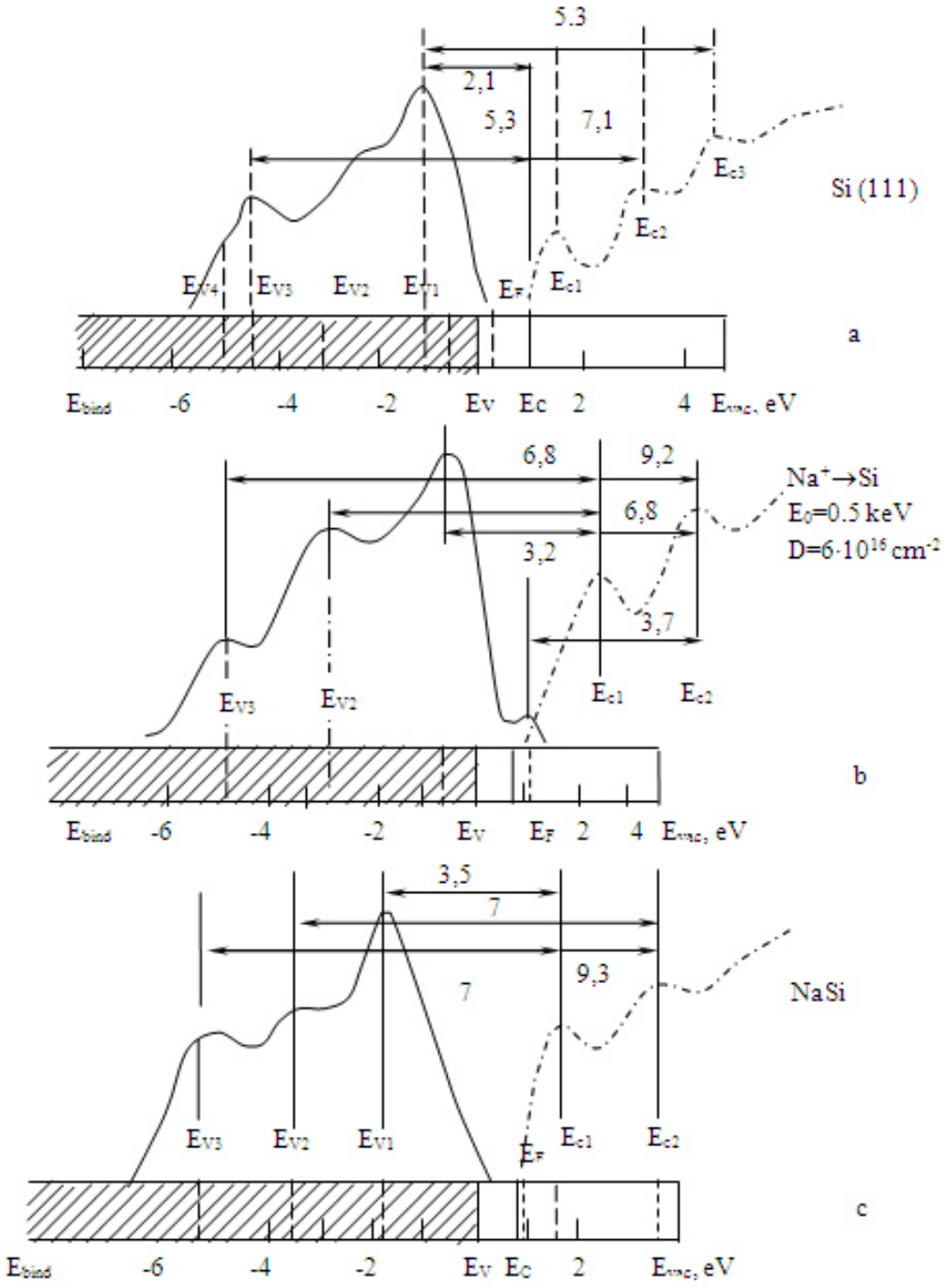

Figure 6. a – Electron - energy diagram of the surface of pure Si – a; Si implanted with Na ions with E_0 = 0.5 keV – b and sodium silicide films NaSi – c.

Table 2 shows the values of the thermionic $e\varphi$ and photoelectron Φ work function, electron affinity χ, and band gap E_g of barium and alkali metal silicides obtained after thermal annealing. The annealing temperature at which surface structures and the type of structures are formed is also given there. As can be seen from the table, annealing of ion - implanted samples leads to the formation of metal silicides with a single crystal structure.

Table 2.
The values of the secondary emission and structural parameters of silicides.

Type of silicide	eφ, eV	Φ, eV	χ, eV	E_g, eV	Type of surface structure	$T_{ann.}$, K
Li Si	2.5	3.2	2.4	0.8	Si(111)-4×4 Li	600
Rb Si	2.65	3.0	2.3	0.7	Si(111)-2×2 Rb	800
Rb Si	2.60	2.8	2.2	0.7	Si(100)-2×4 Rb	750
Cs Si	2.6	3.0	2.2	0.85	Si(111)-4×4 Cs	500
Cs Si	2.3	2.7	2.1	0.80	Si(100)-2×8 Cs	450
Ba Si	2.75	3.1	2.4	0.7	Si(111)-1×1 Ba	900
Ba Si	2.70	3.0	2.5	0.5	Si(100)-2×2 Ba	850
Na Si	2.8	3.2	2.5	0.65	Si(111)-4×4 Na	900
Na Si	2.7	3.1	2.4	0.6	Si(100)-4×4 Na	800
K Si	2.8	3.1	2.5	0.6	Si(100)-2×1 K	750

Conclusion

Thus, the optimal conditions for the formation of thin nanoscale films of barium silicides and alkaline elements were first determined in the work. It was shown that the thickness of metal silicide films increases linearly with increasing energy of implanted ions and at a fixed energy increases with increasing dose as $D^{1/2}$.

Acknowledgments

The work was performed in the framework of program-targeted funding of the Committee of Science of the Ministry of Education and Science of the Republic of Kazakhstan for 2018 - 2020.

References

[1] D. Leong et al., Nature **387** (1997) 686-688.
[2] B. Schuller et al., J. Appl. Phys. **94** (2003) 207-211.
[3] E.A. Shteyman et al., FTT **46** (2004) 26-30. (In Russian)
[4] L. Martinelli et al., Appl. Phys. Lett. **83** (2003) 794-796.
[5] Y. Maeda et al., Thin Solid Films **461** (2004) 160-164.
[6] A.S. Rysbaev, Abstract of a doctoral dissertation Tashkent (2003) 34. (In Russian)
[7] R.I. Batalov et al., FTP **35** (2001) 1320-1325. (In Russian)
[8] R. Bayazitov et al., Nucl. Instrum. Methods. **24** (2005) 224-228.
[9] G.G. Galkin et al., Journal of Technical Physics **78**(2) (2008) 84-90.
[10] T. Suemasu et al., Thin Solid Films **461** (2004) 209-218.
[11] N.I. Plyusnin, Vestnik DVO RAN **5** (2010) 26-34. (In Russian)
[12] L. Chenga, K. Plog, Molecular beam epitaxy and heterostructures (1989) 68-72.
[13] L. Haderbache et al., Thin Solid Films **184** (1990) 317-327.

[14] N.I. Plyusnin, Materials of Electronic Engineering **18**(2) (2015) 81-94.
[15] H.B. Ashurov, Abstract of Doct. Diss. Tashkent (1994) 30. (In Russian)
[16] S.A. Audet, S.E. Wouters, IEEE Trans. Nucl. Sci. **37**(1) (1990) 15-20.
[17] A.S. Rysbaev et al., Abstract 8th International Conference. Almaty, Kazakhstan (2011) 350. (In Russian)
[18] A.S. Rysbaev et al., Surface. **12** (2011) 98-104.
[19] V.I. Fistul, FTP **21**(6) (1987) 1026-1028. (In Russian)
[20] V.A.Uskov et al., M.: Nauka. (1982) 110-114.
[21] I.A. Popov, FTP. **3** (1996) 466-469. (In Russian)
[22] K.P. Gurov, B.A. Kartashkin, Interdifussion in multiphase metal systems (M.: Nauka, 1981) 120-145.
[23] K.P. Gurov, A.M. Gusak, Physics of Metals and Metallurgy. **53**(5) (1982) 842-847. (In Russian)
[24] A.M. Gusak, K.P. Gurov, Phys. Chem. Material Processing. **6** (1982) 109-114.
[25] I.R. Bekpulatov et al., Struktura i fizicheskie svojstva nanorazmernyh plenok silicidov metallov. Monografija (Tashkent: Adabiyot uchqunlari, 2017) 230 p. (in Russian)
[26] A.S. Rysbaev et al., Technical Physics. **59**(10) (2014) 1526-1530.
[27] A.S. Rysbaev et al., E-MRS Spring Meeting, Lille, France (2016) P. 2.8.
[28] A.S. Rysbaev et al., Abstract XLVII International Tulin Conference, Moscow, (2017) 136.
[29] A.S. Rysbaev et al., International Symposium, Tashkent. (2016) 351-352.
[30] A.S. Rysbaev et al., International Symposium, Tashkent. (2016) 235.
[31] V.V. Gorganova, X-ray, electron spectra and chemical bonds (1986) 222-290.